Human Rad51 Protein Requires Higher Concentrations of Calcium Ions for D-loop Formation Than for Oligonucleotide Strand Exchange

Masayuki Takahashi * , Axelle Renodon-Corniere , Tsutomu Mikawa , Naoyuki Kuwabara , Kentaro Ito , Dmitri Levitsky , Hiroshi Iwasaki

Posted Date: 30 January 2024

doi: 10.20944/preprints202401.1991.v1

Keywords: Rad51 protein; homologous recombination; DNA strand exchange; Calcium ion; D-loop formation

Article

Human Rad51 Protein Requires Higher Concentrations of Calcium Ions for D-Loop Formation Than for Oligonucleotide Strand Exchange

Axelle Renodon-Corniere [1], Tsutomu Mikawa [2], Naoyuki Kuwabara [3], Kentaro Ito [4], Dmitri Levitsky [1], Hiroshi Iwasaki [5,6] and Masayuki Takahashi [5,*]

[1] Nantes Université, CNRS, US2B, UMR 6286, Nantes, France
[2] Center for Biosystems Dynamics Research, RIKEN, Yokohama, Japan
[3] High Energy Accelerator Research Organization (KEK), Institute of Materials Structure Science, Structural Biology Research Center, Tsukuba, Japan
[4] Graduate School of Medical Life Science, Yokohama City University, Yokohama, Japan
[5] School of Life Science and Technology, Tokyo Institute of Technology, Tokyo, Japan
[6] Innovative Science Institute, Tokyo Institute of Technology, Yokohama, Japan
* Correspondence: author: Masayuki Takahashi, School of Life Science and Technology, Tokyo Institute of Technology, Tokyo (Japan), takahashi.m.ay@m.titech.ac.jp.

Abstract: Human RAD51 protein (HsRad51)-promoted DNA strand exchange, a crucial step in homologous recombination, is regulated by proteins and calcium ions. The activator protein Swi5-Sfr1 and Ca^{2+} ions stimulate different reaction steps and induce a perpendicular orientation of DNA bases in the presynaptic complex. To investigate the importance of base orientation in the strand exchange reaction, we examined the Ca^{2+} concentration dependence of strand exchange activities and structural changes in the presynaptic complex. Our results show that optimal D-loop formation (strand exchange with closed circular DNA) requires Ca^{2+} concentrations greater than 5 mM, while 1 mM is sufficient for strand exchange between two oligonucleotides. The structural change, which is evidenced by an increase in fluorescence intensity of poly(dεA) (a poly(dA) analog), reaches a plateau at 1 mM Ca^{2+}. Meanwhile, the linear dichroism signal intensity at 260 nm, which is indicative of rigid perpendicular DNA base orientation, requires >2 mM Ca^{2+} for saturation and thus correlates with the stimulation of D-loop formation. Therefore, Ca^{2+} exerts two different effects. Thermal stability measurements suggest that HsRad51 binds two Ca^{2+} ions with K_D values of 0.3 mM and 2.5 mM, implying that one step is stimulated by one Ca^{2+} bond and the other by two Ca^{2+} bonds. We further discuss the parallels between Mg^{2+} activation of RecA and Ca^{2+} activation of HsRad51.

Keywords: Rad51 protein; homologous recombination; DNA strand exchange; calcium ion; D-loop

Introduction

The RAD51 protein, a eukaryotic ortholog of the RecA protein, plays a crucial role in homologous recombination by catalyzing strand exchange between two DNAs of identical sequence [1,2]. This function is important for repairing double-strand breaks, resolving stalled replication forks [3], and facilitating chromosome pair formation during meiosis [4]. In vertebrates, the absence of Rad51 is lethal [5], and mutations in Rad51 or regulatory proteins that lead to defects in homologous recombination increase the risk of cancer in humans [6–9]. *In vivo*, Rad51 activity is tightly regulated by various proteins [10–15], and this regulation also extends to its *in vitro* activity, which is influenced by accessory and regulatory proteins [11,13,16,17]. Notably, both human (HsRad51) and fission yeast Rad51 proteins (SpRad51) are stimulated by Ca^{2+} ions *in vitro* [17,18].

Conversely, frequent overexpression of the human Rad51 protein (HsRad51) in cancer cells has been associated with poor prognosis [9,19–23]. HsRad51 plays a role in counteracting radiotherapy and chemotherapy by repairing DNA damage caused by these treatments, contributing to the

 doi:10.20944/preprints202401.1991.v1

survival of cancer cells [9,21–23]. Inhibition of HsRad51 activity has been proposed as a potential cancer treatment [24,25], leading to the development of inhibitors for HsRad51 [25–27]. A comprehensive understanding of the molecular mechanisms underlying the strand exchange reaction and the regulation of HsRad51 is crucial for drug development and elucidating the complexity of homologous recombination.

Fluorescence resonance energy transfer (FRET)-based real-time analyses of the strand exchange reaction mediated by SpRad51 have revealed a three-step process that follows the formation of the presynaptic complex with single-stranded DNA (ssDNA): (1) the formation of a three-stranded complex (C1 complex) upon homologous binding of double-stranded DNA (dsDNA) to the presynaptic complex; (2) isomerization of the complex, possibly with topological changes in DNA (C2 complex); (3) release of the displaced strand from the filament [17,28].

The activator protein Swi5-Sfr1 and Ca^{2+} promote the perpendicular orientation of ssDNA bases in the presynaptic complex [29,30]. While this base orientation accelerates strand exchange by facilitating the formation of new base pairs, kinetic analyses indicate that Swi5-Sfr1 stimulates the second and third steps, whereas Ca^{2+} primarily stimulates the second step, suggesting distinct mechanisms of stimulation [17]. This study explores the possible connection between the perpendicular base orientation and the stimulation of the strand exchange reaction by examining the Ca^{2+} concentration dependence of structural changes and strand exchange stimulation under identical buffer conditions.

To ensure an accurate comparison, we first identified a buffer condition compatible with all measurements. Strand exchange activity was then assessed using two protocols: (1) strand exchange between two short oligonucleotides and (2) between a single-stranded oligonucleotide and a closed circular dsDNA (D-loop formation). The former is widely used for kinetic analyses with FRET measurements and allows robust assessments [17,28,31], while the latter, closer to *in vivo* conditions, involves topological changes in the closed circular dsDNA. Our observations suggest that higher Ca^{2+} concentrations are required for D-loop formation compared to oligonucleotide strand exchange, suggesting that HsRad51 may bind two Ca^{2+} ions.

We examined the binding stoichiometry by independent measurement and demonstrated Ca^{2+} binding by assessing changes in the thermal stability of HsRad51. The analyses provided support for a stoichiometry of 2 Ca^{2+}/HsRad51.

Subsequently, we examined the Ca^{2+} concentration dependence of structural changes in the presynaptic complex. Measurements of linear dichroism (LD) signal and poly(dεA) fluorescence were performed at different Ca^{2+} concentrations. Poly(dεA) serves as a fluorescent analog of poly(dA), with its fluorescence quenched by collisions between εA bases [32]. The intensity increases upon binding of HsRad51, probably due to the restriction of base movements by HsRad51 [33]. The LD signal at 260 nm is directly associated with the perpendicular orientation of the DNA bases in the complex [29,30,34]. Given the observed aggregate formation of the presynaptic complex at high Ca^{2+} concentrations, we also examined the Ca^{2+} concentration dependence of the light scattering signals [35,36]. Our results suggest that the saturation of LD signal modification and the stimulation of D-loop formation require the binding of two Ca^{2+}. In contrast, one Ca2+ is sufficient to saturate the fluorescence change of poly(dεA) and stimulate the exchange of short oligonucleotide strands.

Notably, Ca^{2+} binding led to a decrease in the thermal stability of HsRad51, similar to how Mg^{2+} affects the thermal stability of RecA [37]. Studies on RecA have shown that Mg^{2+} binds to the C-terminal acidic tail of RecA, preventing its interaction with the RecA core, where DNA binds [37–39]. Mg^{2+} thereby relieves the inhibitory effect of the C-terminal tail and stimulates RecA activity. This suggestion is consistent with the destabilization of RecA by Mg^{2+} and the Mg^{2+}-independent strand exchange activity of C-terminal tail-deleted RecA [38,39]. We discuss the possible similarity of the activation mechanisms of RecA by Mg^{2+} and HsRad51 by Ca^{2+}.

 doi:10.20944/preprints202401.1991.v1

Results

Optimization of experimental conditions

To ensure compatibility of all the experiments, we initially established a reaction condition by excluding bovine serum albumin (BSA) from the buffer to avoid interference with circular dichroism (CD) and fluorescence measurements. However, removing BSA led to decreased reproducibility in the strand exchange reaction, possibly due to defects in the surfaces of Eppendorf tubes promoting spontaneous strand exchange without HsRad51. To counteract this, we tested various detergents and surface coating agents and found that adding a low concentration (0.0075% V/V) of Tween 20 (polyethylene glycol sorbitan monolaurate) significantly improved the reproducibility of the strand exchange reaction and fluorescence measurements. Tween 20 likely prevented the adsorption of Rad51 to the surfaces of quartz cuvettes used for fluorescence measurements.

To minimize interference caused by the binding of Ca^{2+} to free ATP, we reduced the ATP concentration to 300 μM. High ATP concentrations can chelate free Ca^{2+} [40] and interfere with CD measurements due to strong UV absorption. We verified that 300 μM ATP was sufficient for optimal strand exchange without affecting CD measurements. The strand exchange reaction remained unaffected by ATP concentrations ranging from 100–800 μM when experiments were conducted with 1 mM $CaCl_2$. Notably, a slight decrease in strand exchange was observed at 1 mM ATP, likely due to a reduction in Ca^{2+} ion availability for HsRad51.

Furthermore, we introduced sodium hydrochloride (NaCl) (50 mM) to mitigate the nonspecific binding of Ca^{2+} to DNA [41]. Experiments were performed without Mg^{2+} to avoid potential complications arising from the eventual competition and cooperation between the two divalent ions.

Higher Ca^{2+} concentration required for D-loop formation than oligonucleotide strand exchange

We investigated the Ca^{2+} concentration dependence of HsRAD51-mediated D-loop formation and strand exchange between two short oligonucleotides. D-loop formation, involving strand separation of closed circular DNA and being topologically more constrained than short linear DNA, required a higher concentration of Ca^{2+} than oligonucleotide strand exchange. Figure 1 illustrates that the oligonucleotide strand exchange was stimulated with approximately 0.3 mM Ca^{2+} for the half-maximum effect, whereas D-loop formation required 2.5 mM Ca^{2+} for the half-maximum effect. These findings suggest that Ca^{2+} has dual effects on HsRad51, and each HsRad51 protomer binds two Ca^{2+} ions.

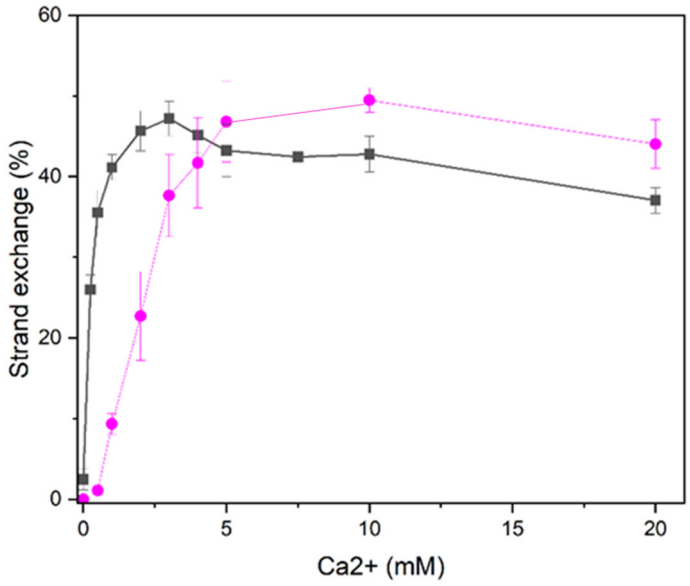

 doi:10.20944/preprints202401.1991.v1

Figure 1. Differential Ca^{2+} concentration dependence for D-loop formation and oligonucleotide strand exchange.

HsRad51-mediated D-loop formation (magenta) and strand exchange between two short oligonucleotides (black) were measured at various Ca^{2+} concentrations.

HsRad51 binds more than two Ca^{2+} ions: thermal denaturation measurements

To determine the binding stoichiometry of Ca^{2+} ions to HsRad51, we conducted thermal denaturation measurements of HsRad51 at various Ca^{2+} concentrations. Ligand binding often alters protein thermal stability [42], as evidenced by the binding of Mg^{2+}, an activating ion for RecA, to RecA, decreasing its thermal stability [37].

The denaturation experiments were performed without any other elements (ATP, DNA) to observe the direct and selective effect of Ca^{2+} on HsRad51. Thermal denaturation was monitored by changes in the CD signal at 222 nm, reflecting alpha-helix content [43]. HsRad51 exhibited a complex denaturation pattern with three apparent transitions: T_{m1} = 38 °C, T_{m2} = 65 °C, and T_{m3} = 90 °C in the absence of Ca^{2+} (Fig. 2A), possibly corresponding to the independent unfolding of three domains in HsRad51. Structural analyses of Rad51 by X-ray crystallographic studies have shown that HsRad51 comprises small N-terminal and C-terminal domains and a large core domain [44,45].

Ca^{2+} was found to decrease the thermal stability of HsRad51 (Fig. 2). The lowering of the first transition temperature (T_{m1}) occurred with less than 1 mM Mg^{2+} (Figs. 2B and 2C). The concentration of Ca^{2+} required for the half-maximum effect was approximately 0.2 mM (Fig. 2C). In contrast, changes in the second and third transition temperatures (T_{m2} and T_{m3}) required higher Ca^{2+} concentrations for saturation (Figs. 2A and 2D). The concentration for the half-maximum effect on the second transition was approximately 2.5 mM (Fig. 2D). These results suggest that HsRad51 binds two Ca^{2+} ions per protomer with K_{D1} = 0.2 mM and K_{D2} = 2.5 mM. While the stimulation of oligonucleotide strand exchange requires the binding of only one Ca^{2+}, D-loop formation requires the binding of two Ca^{2+}.

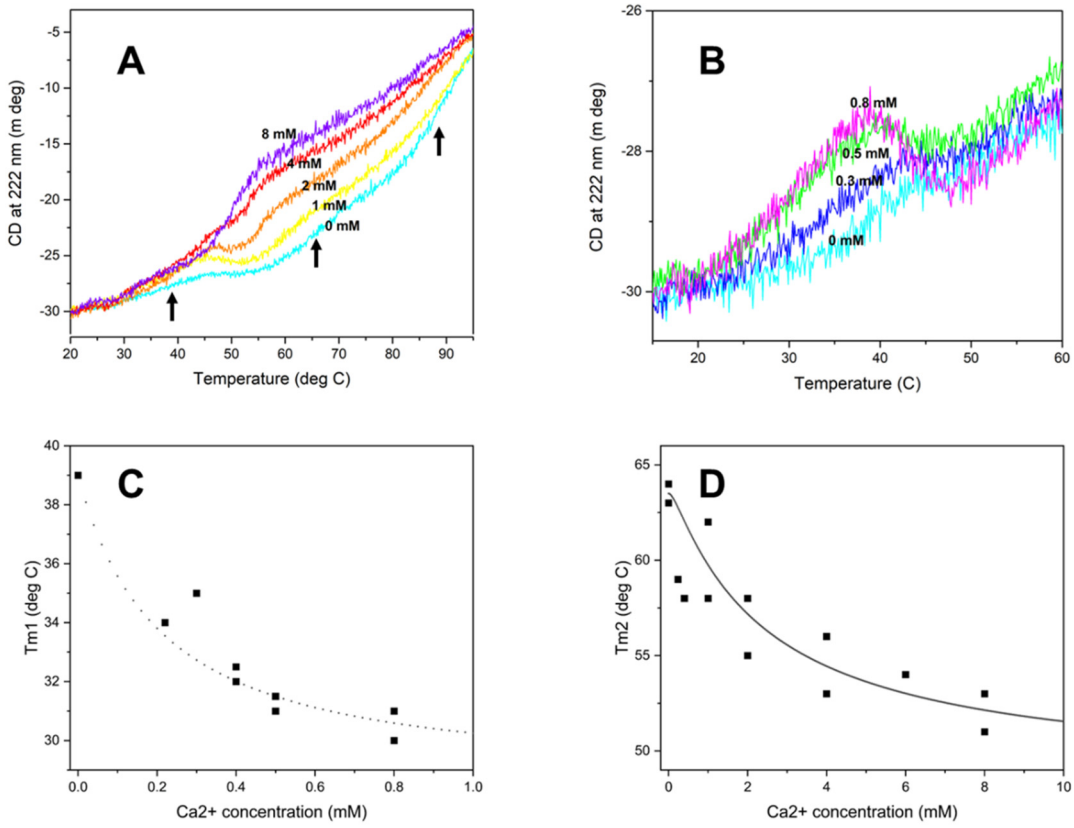

 doi:10.20944/preprints202401.1991.v1

Figure 2. Ca^{2+} concentration dependence of HsRad51 thermal denaturation. (A) Ca^{2+} binding of HsRad51 was evaluated by measuring its thermal denaturation at different Ca^{2+} concentrations, as noted in the figure. The denaturation was monitored by measuring changes in the CD signal at 220 nm following temperature elevation. Three fleshes indicate the three transitions. (B) Detailed changes in the denaturation profile with increasing Ca^{2+} concentrations (0–0.8 mM) are shown. (C) Change in the T_m of the first transition (T_{m1}) with Ca^{2+} concentrations. A theoretical curve generated with K_{D1} = 0.2 mM and K_{D2} = 2.5 mM is shown. (D) Change in the T_m of the third transition (T_{m3}) with Ca^{2+} concentrations. A theoretical curve generated with K_{D1} = 0.2 mM and K_{D2} = 2.5 mM is shown.

Saturation of poly(dεA) fluorescence change requires less than 1 mM Ca^{2}

To investigate the Ca^{2+}-promoted structural changes in the presynaptic complex, we measured the fluorescence of the poly(dA) analog, poly(dεA). The fluorescence intensity of poly(dεA) is much lower than that of monomeric εA nucleobase due to base/base collisions and stacking [32,33]. The binding of HsRad51 to poly(dεA) increased the fluorescence intensity of poly(dεA) in a Ca^{2+} concentration-dependent manner (Fig. 3). The change plateaued at a Ca^{2+} concentration of less than 1 mM. The concentration of Ca^{2+} required to reach the half-maximum effect was 0.2 mM. Mg^{2+} ion, which activates less HsRad51, increased the fluorescence intensity of poly(dεA) to a lesser extent, indicating this fluorescence change would be related to the activation of the strand exchange reaction. Therefore, the binding of one Ca^{2+} ion is sufficient to increase the fluorescence intensity of poly(dεA), attributed to a decrease in base/base collisions caused by the restriction of DNA base motion by HsRad51 in the presence of Ca^{2+}.

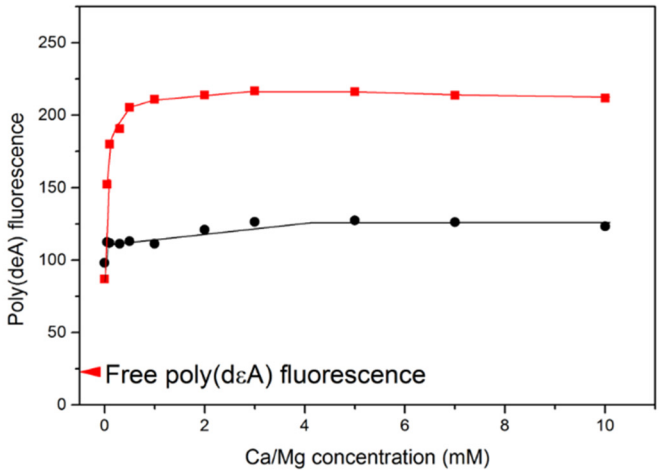

Figure 3. Effect of Ca^{2+} on the poly(dεA) fluorescence intensity.

The fluorescence intensity of poly(dεA) in the HsRad51-ATP filament was measured at various Ca^{2+} (red symbols) or Mg^{2+} concentrations (black symbols).

More than 2 mM of Ca^{2+} was required to saturate the LD signal

We performed flow LD measurements of the HsRad51-ssDNA-ATP filament at different Ca^{2+} concentrations. In flow LD, a shear force is applied to align sample molecules, and the difference in absorption between light polarized parallel to the sample orientation axis and light polarized perpendicular to the axis was measured [34]. Flow LD provides information about the chromophore orientation relative to the filament axis, and the signal intensity depends on the degree of filament

 doi:10.20944/preprints202401.1991.v1

orientation itself with respect to its stiffness [34]. Only non-moving chromophores in a stiff filament result in a significant LD signal [34].

The LD spectrum of the HsRad51 presynaptic complex contains information regarding the orientation of all chromophores in the complex, *i.e.*, DNA bases, ATP, and tyrosine residues of HsRad51 [29,30,34]. The signal around 260 nm is dominated by DNA and reflects DNA base orientation. Signals around 230 and 280 nm primarily indicate the tyrosine residue orientations of HsRad51 [29,30,34]. Our prior experiments showed that HsRad51 binding to ssDNA in the presence of Mg^{2+} and ATP exhibited LD signal, showing the formation of stiff filament. However, the LD spectrum showed no significant signal from the DNA [29,30], suggesting local movements or random orientations of the DNA bases. In contrast, Ca^{2+} induces a large negative LD signal from DNA bases, indicating the perpendicular orientation of DNA bases relative to the filament axis in the presence of Ca^{2+} [30].

At various Ca^{2+} concentrations, we measured the LD spectra of the HsRad51/poly(dT)/ATP complex (Fig. 4A). No LD signal was observed in the absence of Ca^{2+} (and Mg^{2+}), suggesting that stiff filaments were not formed without divalent ion. A negative LD signal at 260 nm appeared at 0.4 mM Ca^{2+} and intensified with increasing Ca^{2+} concentrations up to 2 mM (Figs. 4A and 4B). The results showed that 1 mM Ca^{2+} was insufficient to produce a maximum change in LD signal intensity at 260 nm, contrasting the effect of 1 mM Ca^{2+} on the fluorescence of poly(dεA). The LD signal decreased at 3 mM Ca^{2+} and almost disappeared at 5 mM Ca^{2+}, certainly due to aggregate formation (Fig. 4B). Estimation of the Ca^{2+} concentration for the half-maximum effect on the LD signal change was therefore difficult. However, the requirement of more than 2 mM Ca^{2+} for the maximum signal change suggests that the binding of 2 Ca^{2+} ions is needed for the LD signal modification.

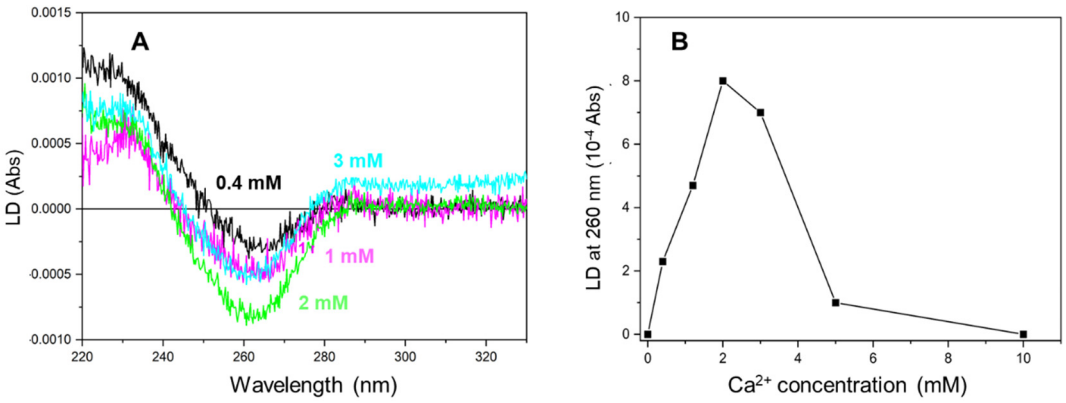

Figure 4. LD spectra of the ATP-poly(dT)-HsRad51 complex at various Ca^{2+} concentrations. (a) The LD spectra of the ATP-poly(dT)-HsRad51 complex were recorded at various Ca^{2+} concentrations, as indicated in the figure. (B) The LD signal intensity at 260 nm was plotted as a function of Ca^{2+} concentration.

The change in LD signal may result from a modification in the structure or the stiffness of the filamentous molecule. Stiffness-related modification changes the intensity of the LD signal without altering the spectral shape. Ca^{2+} modified the spectral shape: the ratio of the LD signal at 260 nm to that at 230 nm changed with increasing Ca^{2+} concentrations, suggesting that Ca^{2+} alters the structure of the synaptic complex, possibly resulting in better aligned DNA bases.

The decrease in signal intensity at Ca^{2+} concentrations higher than 3 mM may be associated with the reduced orientation of the presynaptic filament due to aggregate formation, supported by the increase in light-scattering-related signals above 300 nm.

 doi:10.20944/preprints202401.1991.v1

Light scattering promoted at high Ca^{2+} concentrations

We subsequently examined the aggregate state of the presynaptic complex by performing light scattering, which increases with molecular size and can be used to detect aggregate formation [35,36].

Light scattering was more pronounced at Ca^{2+} concentrations above 3 mM (Fig. 5) and correlated with the decrease in the HsRad51 activation observed at high Ca^{2+} concentrations (Fig. 1).

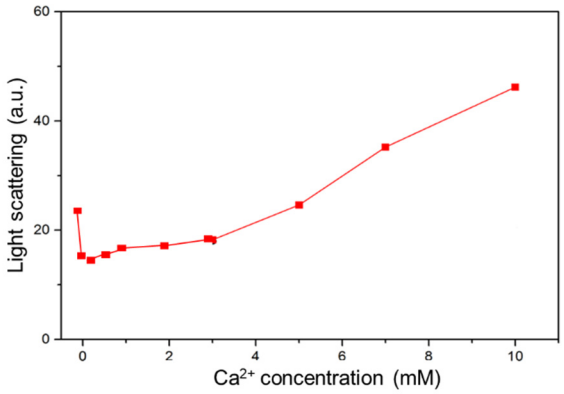

Figure 5. Light scattering of the ATP-poly(dT)-HsRad51 complex at various Ca^{2+} concentrations.

Light scattering of the ATP-poly(dT)-HsRad51 complex with various Ca^{2+} concentrations was measured at 400 nm. Relative signal intensity was plotted as a function of Ca^{2+} concentration.

DISCUSSION

To elucidate the molecular mechanisms controlling Ca^{2+}-mediated activation of HsRad51, we examined HsRad51/Ca^{2+} interactions, Ca^{2+}-dependent structural changes in the presynaptic complex, and HsRad51 activities under uniform reaction conditions. Our findings suggest that HsRad51 binds two Ca^{2+} molecules. The binding of one Ca^{2+} is sufficient to stimulate strand exchange between two short oligonucleotides and to restrict DNA base movements. The second Ca^{2+} binding stimulated D-loop formation and promoted the perpendicular alignment of DNA bases in the presynaptic complex. New questions include how Ca^{2+} induces the perpendicular alignment of DNA bases and why the formation of a D-loop requires a higher concentration of Ca^{2+}. These results also have parallels with Rad51 activation by Swi5/Sfr1 and RecA activation by Mg^{2+} ions.

Similarity with the activation of strand exchange by Swi5-Sfr1 protein

Ca^{2+} specifically stimulates the C1 to C2 transition step of the reaction and slows the release of the displaced strand [17,28]. In contrast, Swi5-Sfr1 accelerates the release of the displaced strand release and the transition from C1 to C2, indicating some difference in the activation mechanism [17,28]. However, both facilitate the perpendicular orientation of DNA bases in the presynaptic complex [29,30] and accelerate the C1 to C2 transition. The perpendicular orientation of DNA bases facilitates base pair formation with the complementary strand and accelerates the strand exchange reaction. The different effect on the strand displacement step between Swi5-Sfr1 and Ca^{2+} is likely due to a different mechanism, possibly related to ATP hydrolysis. Swi5-Sfr1 increases the ATPase activity of Rad51, while Ca^{2+} inhibits it [17,18].

The need for higher Ca^{2+} concentrations to stimulate D-loop formation may be attributed to the difficulty of inducing base-pair opening in closed circular DNA than in short linear dsDNA [46]. Base-pair opening of closed circular DNA leads to topological constraints. The opening of closed circular DNA probably occurs rarely or for short-period of time. The ssDNA should be ready to pair

 doi:10.20944/preprints202401.1991.v1

with it. The perpendicular base orientation is required. Our preliminary experiments with SpRad51 show that maximal stimulation of the C1 to C2 transition requires more than 5 mM Ca^{2+}, supporting the requirement of two Ca^{2+} for this step and the association of this step with a topological change in DNA. It would be informative to examine whether the concentrations of Swi5/Sfr1 needed to stimulate D-loop formation exceed the concentrations required for oligonucleotide strand exchange, similar to the observations with Ca^{2+}.

Potential Ca^{2+}-binding site at the N-terminal extremity of HsRad51

To better understand the activation mechanism, we first searched potential Ca^{2+}-binding sites, by locating a cluster of acidic negatively charged residues. In the case of RecA, Mg^{2+} binds to the acidic residue cluster at the C-terminal tail [38]. We observed a small cluster of acidic residues in the N-terminal end (from residue 8 to 18) (Fig. 6). To confirm this suggestion, we compared the amino acid sequence of HsRad51 with those of SpRad51 and budding yeast Rad51 (ScRad51). Ca^{2+} stimulates SpRad51 [17,28] but not ScRad51 [18]. We expected some difference in the amino acid sequence of Ca^{2+}-binding site between HsRad51 and ScRad51. Their overall sequences are well conserved except for the N-terminal end (Fig. 6). ScRad51 has a longer N-terminal end than HsRad51 and SpRad51. This difference supports the idea that Ca^{2+} binds at the N-terminal end of HsRad51. This part is important for the regulation of Rad51. N-terminal acetyltransferase NatB regulates Rad51 [47]. Phosphorylation at positions 13 and 14 regulates Rad51 [48]. We prepare a HsRad51 lacking the N-terminal end to test our hypothesis. However, this cluster of acidic residues is too small to bind two Ca^{2+} ions. There would be another Ca^{2+}-binding site.

Figure 6. A cluster of negatively charged amino acid residues at the N-terminal of HsRad51.

The amino acid sequence of HsRad51 is shown in comparison with that of SpRad51 and ScRad51. Negatively charged residues are indicated in magenta.

Similarity with the activation of RecA-promoted strand exchange by Mg^{2+}

In parallel with the effect of Mg^{2+} on RecA, Ca^{2+} reduces the thermal stability of HsRad51. Typically, ligand binding increases the thermal stability of protein [42]. This unusual effect of divalent ions on RecA and HsRad51 implies a common activation mechanism. Mg^{2+} binds to the C-terminal acidic tail of RecA, preventing its interaction with the core of RecA, where DNA binding occurs [37–39]. RecA lacking the C-terminal tail becomes insensitive to the Mg^{2+} concentration for thermal stability and strand exchange activity [37–39]. Thus, Mg^{2+} alleviates the inhibitory effect of the C-terminal tail and stimulates RecA activity.

It is possible that Ca^{2+} binds at the N-terminal end and prevents its interaction with the DNA-binding site. The interaction of the N-terminal end with the DNA-binding site would hinder the formation of the stable presynaptic complex. DNA may quickly dissociate from and reassociate to Rad51. This unstable binding allows movements of the DNA backbone and bases. This slows the formation of new base pairs, an important step of the strand exchange reaction. Ca^{2+} may release this inhibitory effect of N-terminal end and promote a close interaction between DNA and HsRad51. Burgreev and Mazin reported stabilization of the presynaptic complex by Ca^{2+} [18]. Ca^{2+} may strengthen the contact between DNA and HsRad51 and immobilize the DNA bases. The increase in

 doi:10.20944/preprints202401.1991.v1

fluorescence intensity of poly(dεA) and the strong negative LD signal at 260 nm by Ca^{2+} showed the restriction of DNA base movements. The binding of one Ca^{2+} may not be sufficient to completely stabilize the presynaptic complex and immobilize the DNA bases.

We investigate the validity of this explanation by experiments and molecular simulations. Interestingly, Swi5-Sfr1 dimer also stabilizes the presynaptic complex by slowing down the dissociation rate [17,28]. Although Ca^{2+} may not play a regulatory role in vivo [49], understanding its action clarifies the action of biological regulatory elements.

MATERIALS AND METHODS

Materials

Poly(dT), poly(dA), ATP, and Tween-20 were obtained from Sigma-Aldrich. HsRad51 was purified according to the procedure described in [50]. Poly(dεA) was synthesized by chemical modification of poly(dA) using chloroacetaldehyde (Aldrich), according to the method described [51]. The degree of modification was determined spectroscopically to be approximately 93%, using the formula provided by Ledneva et al. [52]. Concentrations were determined based on UV absorption, utilizing the following extinction coefficients: ε_{263} nm = 8520 M^{-1} cm^{-1} for poly(dT), ε_{257} nm = 3800 M^{-1} cm^{-1} for poly(dεA), and ε_{260} nm = 15400 $M^{-1}cm^{-1}$ for ATP.

Experimental conditions

Experiments were performed in a buffer containing 30 mM Tris/hydrochloric acid (pH 7.5), 50 mM NaCl, 0.1 mM ethylenediamine tetraacetic acid (EDTA), 0.07% Tween 20, and the specified concentrations of Ca^{2+}. ATP concentration, if present was maintained at 300 μM. In the text, the concentration of free Ca^{2+} (after deduction of 0.1 mM Ca^{2+} chelated by EDTA) is given without additional mention. Tween-20 was added to prevent the adsorption of HsRad51 on the surface of the quartz cell or plastic tube.

LD measurements

LD spectra were recorded with a Jasco J-810 CD spectrometer in step mode (data interval: 0.1 nm; time constant: 0.175 s; bandwidth: 2 nm) and LD mode. The samples were aligned using a mini-Couette cell (Jasco Europe), and the baseline was determined by slowly rotating the Couette cell filled with the sample to average defects in the cell.

CD measurements of thermal unfolding

Thermal unfolding of HsRad51 was monitored by tracking the change in the CD signal at 222 nm (bandwidth, 5 nm; data interval, 0.1°C; time constant, 2 s) with temperature elevation (1°C/min). A mini-cuvette of 1 × 0.2 cm (Hellman) with a path length of 1 cm was utilized in these measurements. The temperature was controlled with a Peltier effect controller.

Fluorescence measurements

The fluorescence of poly(dεA) was measured with a Jasco FP-8300 fluorometer. The emission signal at 380 nm (bandwidth: 10 nm) was recorded upon excitation at 320 nm (bandwidth: 5 nm). The results from 20 measurements were averaged, and the temperature was kept at 20°C using a Peltier effect controller.

Strand exchange and D-loop formation

DNA strand exchange between two short oligonucleotides was performed as described in [30].

Author Contributions: A. R-C. prepared HsRad51 and performed strand exchange reactions**;** T. M. measured LD and CD and analyzed the results; N. K. prepared HsRad51 and conducted preliminary LD and CD measurements; K. I. measured the fluorescence values and participated in experimental design; D. L. proposed

the project and analyzed Ca^{2+}-binding sites; H. I. designed the experiments; M. T. designed the experiments, analyzed the data, and wrote the manuscript. All authors contributed to writing the manuscript.

References

1. Shinohara, A.; Ogawa, H.; Matsuda, Y.; et al. Cloning of human, mouse and fission yeast recombination genes homologous to RAD51 and recA. *Nat Genet*, **1993**, 4, 239–243.
2. Baumann, P.; West, S.C. Role of the human RAD51 protein in homologous recombination and double-stranded-break repair. *Trends Biochem Sci*. **1998**, 23, 247-251.
3. Anand, R.; Beach, A.; Li, K.; Haber, J. Rad51-mediated double-strand break repair and mismatch correction of divergent substrates. *Nature*, **2017**, 544, 377–380.
4. Gerton, J.; Hawley, R. Homologous chromosome interactions in meiosis: diversity amidst conservation. *Nat Rev Genet*, **2005**, 6, 477–487.
5. Tsuzuki. T.; Fujii, Y.; Sakumi, K.; Tominaga, Y.: Nakao, K.; Sekiguchi, M.; Matsushiro, A.; Yoshimura, Y.; Morita, T. Targeted disruption of the Rad51 gene leads to lethality in embryonic mice. *Proc Natl Acad Sci USA*. **1996**, 93, 6236-40.
6. Bindra RS, Schaffer PJ, Meng A, Woo J, Måseide K, Roth ME, Lizardi P, Hedley, D.W.; Bristow, R.G.; Glazer, P.M. Down-regulation of Rad51 and decreased homologous recombination in hypoxic cancer cells. *Mol. Cell. Biol*. **2004**, 24, 8504–8518.
7. Bishop, A.J.R.; Schiestl, R.H. Homologous recombination and its role in carcinogenesis. *J. Biomed. Biotech*. **2002**, 2, 75–85.
8. Heeke AL, Pishvaian MJ, Lynce F, Xiu J, Brody JR, Chen WJ, Baker TM, Marshall JL.; Isaacs, C. Prevalence of homologous recombination related gene mutations across multiple cancer types. *JCO Precision Oncology*, **2018**, 2, 1– 13.
9. Wang Z, Jia R, Wang L, Yang Q, Hu X, Fu Q, Zhang X, Li W, Ren Y. The Emerging Roles of Rad51 in Cancer and Its Potential as a Therapeutic Target. *Front Oncol*. **2022**, 935593.
10. Sung, P. Function of yeast Rad52 protein as a mediator between replication protein A and the Rad51 recombinase. *J. Biol. Chem*. **1997**, 272, 28194–28197.
11. Sung, P. Yeast Rad55 and Rad57 proteins form a heterodimer that functions with replication protein A to promote DNA strand exchange by Rad51 recombinase. *Genes Dev*. **1997**, 11, 1111–1121.
12. Sung, P.; Krejci, L.; Van Komen, S.; Sehorn, M.G. Rad51 recombinase and recombination mediators. *J. Biol. Chem*. **2003**, 278, 42729–42732.
13. Jensen, R. B., Carreira, A. & Kowalczykowski, S. C. Purified human BRCA2 stimulates RAD51-mediated recombination. *Nature* **2010**, 467, 678–683.
14. Akamatsu, Y., Dziadkowiec, D., Ikeguchi, M., Shinagawa, H. & Iwasaki, H. Two different Swi5-containing protein complexes are involved in mating-type switching and recombination repair in fission yeast. *Proc. Natl. Acad. Sci. USA*, **2003**, 100, 15770–15775.
15. Akamatsu, Y. et al. Fission yeast Swi5/Sfr1 and Rhp55/Rhp57 differentially regulate Rhp51-dependent recombination outcomes. *EMBO J*. **2007**, 26, 1352–1362.
16. Haruta, N. et al. The Swi5-Sfr1 complex stimulates Rhp51/Rad51- and Dmc1-mediated DNA strand exchange in vitro. *Nat. Struct. Mol. Biol*. **2006**, 13, 823–830.
17. Ito K, Murayama Y, Takahashi M & Iwasaki H. Two three-strand intermediates are processed during Rad51-driven DNA strand exchange. *Nature Struct. & Mol. Biol.* **2018**, 25, 29-36.
18. Bugreev, D.V. and Mazin, A.V. Ca^{2+} activates human homologous recombination protein Rad51 by modulating its ATPase activity. *Proc. Natl. Acad. Sci. U.S.A*. **2004**, 101, 9988–9993.
19. Morrison C, Weterings E, Mahadevan D, Sanan A, Weinand M, Stea B, et al. Expression levels of RAD51 inversely correlate with survival of glioblastoma patients. *Cancers*, **2021**, 13, 5358.
20. Qiao GB, Wu YL, Yang XN, Zhong WZ, Xie D, Guan XY, et al. High-Level expression of Rad51 is an independent prognostic marker of survival in non-small-cell lung cancer patients. *Br J Cancer*, **2005**, 93, 137–43.
21. King, H. O.; Brend, T.; Payne, H. L.; Wright, A.; Ward, T. A.; Patel, K.; Egnuni, T.; Stead, L. F.; Patel, A.; Wurdak, H.; Short, S. C. RAD51 is a selective DNA repair target to radiosensitize glioma stem cells. *Stem Cell Reports*, **2016**, 8, 125-139.
22. Gachechiladze, M., Škarda, J., Soltermann, A., & Joerger, M. RAD51 as a potential surrogate marker for DNA repair capacity in solid malignancies. *International Journal of Cancer*, **2017**, 141, 1286-1294.
23. Orhan, E.; Velazquez, C.; Tabet, I.; Sardet, C.; Theillet, C. Regulation of RAD51 at the transcriptional and functional levels: What prospects for cancer therapy? *Cancers (Basel)*, **2021**, 13, 2930.

24. Taki, T.; Ohnishi, T.; Yamamoto, A.; Hiraga, S.; Arita, N.; Izumoto, S.; Hayakawa, T.; Morita, T. Antisense inhibition of the RAD51 enhances radiosensitivity. *Biochemical and Biophysical Research Communications*, **1996**, 223, 434-438.
25. Ward, A.; Khanna, K.K.; Wiegmans, A.P. Targeting homologous recombination, new pre-clinical and clinical therapeutic combinations inhibiting RAD51. *Cancer Treatment Reviews*, **2014**, 41, 35-45.
26. Grundy, M.K.; Buckanovich, R. J.; Bernstein, K. A. Regulation and pharmacological targeting of RAD51 in cancer. *NAR Cancer*, **2020**, 2, 1-14.
27. Demeyer, A.; Benhelli-Mokrani, H.; Chénais, B.; Weigel, P.; Fleury, F. Inhibiting homologous recombination by targeting RAD51 protein. *Biochim Biophys Acta Rev Cancer*. **2021**, 1876, 188597.
28. Ito, K.: Murayama, Y.; Kurokawa, Y.; Kanamaru, S.; Kokabu, Y.; Maki, T.; Mikawa, T.; Argunhan, B.; Tsubouchi, H.; Ikeguchi, M.; Takahashi, M.; Iwasaki, H. Real-time tracking reveals catalytic roles for the two DNA binding sites of Rad51. *Nature Communications*, **2020**, 11, 1-17.
29. Fornander, L.H.; Renodon-Corniere, A.; Kuwabara, N.; Ito, K.; Tsutsui, Y.; Shimizu, T.; Iwasaki, H.; Norden, B.; Takahashi, M. Swi5-Sfr1 protein stimulates Rad51-mediated DNA strand exchange reaction through organization of DNA bases in the presynaptic filament. *Nucl. Acids Res*. **2014**, 42, 2358–2365.
30. Fornander, L.H.; Frykholm, K.; Reymer, A.; Renodon-Cornière, A.; Takahashi, M.; Nordén, B. Ca^{2+} improves organization of single-stranded DNA bases in human Rad51 filament, explaining stimulatory effect on gene recombination. *Nucl. Acids Res*. **2012**, 40, 4904-4913.
31. Bazemore, L.R.; Takahashi, M.; Radding, C.M. Kinetic analysis of pairing and strand exchange catalyzed by RecA: Detection by fluorescence energy transfer. *J. Biol. Chem*. **1997**, 272, 14672-14682.
32. Barker, B.M.; Vanderkooi, J.; Kallenbach, N.R. Base stacking in a fluorescent dinucleoside monophosphate: εApεA, *Biopolymers*, **1978**, 17, 1361-1372
33. Chabbert, M.; Lami, H.; Takahashi, M. Cofactor-induced orientation of the DNA bases in single-stranded DNA complexed with RecA protein. A fluorescence anisotropy and time-decay study. *J. Biol. Chem*. **1991**, 266, 5395-5400.
34. Takahashi, M.; Norden, B. Linear dichroism measurements for the study of protein-DNA interactions. *Int. J. Mol. Sci*. **2023**, 24, 16092.
35. Minton, A.P. Recent applications of light scattering measurement in the biological and biopharmaceutical sciences. *Anal. Biochem*. **2016**, 501, 4-22.
36. Murphy, R.M. Static and dynamic light scattering of biological macromolecules: what can we learn? *Current Opinion in Biotechnology*, **1997**, 8, 25-30
37. Kim R, Kanamaru S, Mikawa T, Prevost C, Ishii K, Ito K, Uchiyama S, Oda M, Iwasaki H, Kim SK & Takahashi M. RecA requires two molecules of Mg2+ ions for its optimal strand exchange activity in vitro. *Nucl. Acids Res*, **2018**, 46, 2548–2559.
38. Lusetti, S.L.; Shaw, J.J.; Cox, M.M. Magnesium ion-dependent activation of the RecA protein involves the C terminus. *J. Biol. Chem*. **2003**, 278, 16381–16388.
39. Fan, H.F.; Su, S. The regulation mechanism of the C-terminus of RecA proteins during DNA strand-exchange process. *Biophys J*. **2021**, 120, 3166-3179.
40. John E. Wilson, Arnold Chin, Chelation of divalent cations by ATP, studied by titration calorimetry, *Anal. Biochem*. **1991**, 193, 16-19.
41. Nikolay Korolev, Alexander P. Lyubartsev, Allan Rupprecht, and Lars Nordenskiöld, L. Competitive binding of Mg^{2+}, Ca^{2+}, Na^{+}, and K^{+} ions to DNA in oriented DNA fibers: Experimental and Monte Carlo simulation results. *Biophys. J*. **1999**, 77, 2736-2749.
42. Celej, M.S.; Montich, G.G.; Fidelio, G.D. Protein stability induced by ligand binding correlates with changes in protein flexibility. *Protein Science*, **2003**, 12, 1496-1506.
43. Greenfield N.J. Using circular dichroism spectra to estimate protein secondary structure. *Nat Protoc*. **2006**, 1, 2876-90.
44. Conway, A.; Lynch, T.; Zhang, Y. et al. Crystal structure of a Rad51 filament. *Nat Struct Mol Biol* **2004**, 11, 791–796.
45. Pellegrini, L. et al. Insights into DNA recombination from the structure of a Rad51-BRCA2 complex. *Nature* **2002**, 420:287–293.
46. Vinograd, J.; Lebowitz, J.; Watson, R. Early and late helix-coil transitions in closed circular DNA the number of superhelical turns in polyoma DNA. *J. Mol. Biol.* **1968**, 33, 173-197.
47. Sugaya, N.; Tanaka, S.; Keyamura, K.; Noda, S.; Akanuma, G.; Hishida, T. N-terminal acetyltransferase NatB regulates Rad51-dependent repair of double-strand breaks in Saccharomyces cerevisiae. *Genes Genet Syst*. **2023**, 98, 61-72.
48. Yata, K.; Lloyd, J.; Maslen, S.; Bleuyard, J.Y.; Skehel, M.; Smerdon, S.J.; Esashi, F. Plk1 and CK2 act in concert to regulate Rad51 during DNA double strand break repair. *Molecular cell*. **2012**, 45, 371-83.

 doi:10.20944/preprints202401.1991.v1

49. Nimonkar, A.V.; Dombrowski, C.C.; Siino, J.S.; Stasiak, A.Z.; Stasiak, A.; Kowalczykowski, S.C. Saccharomyces cerevisiae Dmc1 and Rad51 proteins preferentially function with Tid1 and Rad54 proteins, respectively, to promote DNA strand invasion during genetic recombination. *J. Biol. Chem*. **2012**, 287, 28727–2873
50. Matsuo, Y.; Sakane, I.; Takizawa, Y.; Takahashi, M.; Kurumizaka, H. Roles of the human Rad51 L1 and L2 loops in DNA binding. *FEBS J*. **2006**, 273, 3148-3159
51. Cazenave, C.; Toulme, J.J.; Hélène, C. Binding of RecA protein to single-stranded nucleic acids: spectroscopic studies using fluorescent polynucleotides. *EMBO J*. **1983**, 2, 2247-51.
52. Ledneva, R.K.; Razjivin, A.P.; Kost, A.A.; Bogdanov, A.A. Interaction of tobacco mosaic virus protein with synthetic polynucleotides containing a fluorescent label: optical properties of poly(A,epsilonA) and poly(C,epsilonC) copolymers and energy migration from the tryptophan to 1,N6-ethenoadenine or 3,N4-ethenocytosine residues in RNP. *Nucleic. Acids Res.* **1978**, 5, 4225-43.